MIT Open Access Articles

Stabilizing a Vehicle near Rollover: An Analogy to Cart-Pole

Massachusetts Institute of Technology

Stabilizing a Vehicle near Rollover: An Analogy to Cart-Pole Stabilization

Steven C. Peters, James E. Bobrow, and Karl Iagnemma

Abstract—An analogy between the dynamics of a cart-pole system and vehicle rollover dynamics is used to derive a controller for tipping up and stabilizing a planar model of a passenger vehicle near rollover by controlling lateral tire friction forces. The controller is based on a previously published controller for stabilizing a cart-pole using partial feedback linearization and energy shaping. A necessary condition for tip-up is given based on the surface friction coefficient and the location of the vehicle center of gravity (c.g.). A multi-body vehicle model with suspension is presented in the form of the robotic manipulator equations. Simulation results are presented demonstrating the effect of friction and suspension properties on the tip-up problem.

I. INTRODUCTION

A significant amount of research and development effort over the past 40 years has been devoted to improving the safety of passenger vehicles. Despite these efforts, in the United States in 2004 more than 40,000 people were killed and 2.5 million injured in motor vehicle accidents, at an estimated economic cost of $200 billion. Of these accidents, rollover is particularly fatal, accounting for more than 9000 deaths and 200,000 injuries. Rollovers constituted just 2.3% of total accidents but over 10% of fatal accidents, and trailed only head-on collisions and collisions with pedestrians in this unfortunate ratio [1].

Significant research effort has been devoted to detecting and preventing rollover through active control. Numerous approaches attempt to detect or predict wheel lift-off using on board sensing and use a combination of automatic steering and braking to keep the wheels on the ground [2, 3, 4]. Several methods use a concept of "roll energy" to predict if wheel lift-off will occur or if the vehicle will tip over [5, 6]. One method has been developed into a commercially available rollover stability control system [7].

One challenging aspect of the control of vehicle rollover dynamics is the presence of more degrees of freedom than control inputs. Note that this is the definition of an underactuated system. Numerous approaches exist for the control of underactuated systems, which are often demonstrated on canonical problems, such as swing-up or stabilization of an Acrobot or cart-pole in the inverted

position [8, 9, 10].

An analogy can be made between the cart-pole and a vehicle during rollover since the dynamics of each system are similar. The control problem of swinging up and stabilizing the cart-pole is similar to tipping up a vehicle onto two wheels and stabilizing it with its c.g. balanced directly above the wheels. A controller that solves the vehicle tip-up stabilization problem would provide a powerful demonstration of controllability during tip-up. This level of controllability could be applied to other control problems, such as safely returning a vehicle to the ground after inadvertent tip-up or navigating robots for which driving on two wheels is an additional mobility mode.

This paper presents a controller for tipping up a vehicle based on a controller for swing-up of the cart-pole utilizing partial feedback linearization and energy shaping [8]. In Section II, a brief review of cart-pole dynamics and an intuitive swing-up controller are presented. In Section III, a model of vehicle rollover dynamics is presented and compared to the cart-pole dynamics. A controller for vehicle tip-up is derived based on the cart-pole swing-up controller. In Section IV, simulation results demonstrating tip-up of the controller are shown, followed by a discussion of the results.

II. DYNAMICS AND SWING-UP CONTROL OF THE CART-POLE

A. Cart-pole dynamics

The cart-pole is a mechanical system consisting of a pendulum attached to a cart that rolls freely on a flat surface, as shown in Fig. 1. The cart-pole has two degrees of freedom, the cart position x and the pendulum angle θ, and one input, the force u acting on the cart. The dynamics of the cart pole are given below, where the cart has mass M and the pendulum has mass m, moment of inertia I, and c.g. displacement l.

$$\begin{bmatrix} M+m & -ml\cos\theta \\ -ml\cos\theta & I+ml^2 \end{bmatrix}\begin{bmatrix} \ddot{x} \\ \ddot{\theta} \end{bmatrix} + \begin{bmatrix} 0 & ml\dot{\theta}\sin\theta \\ 0 & 0 \end{bmatrix}\begin{bmatrix} \dot{x} \\ \dot{\theta} \end{bmatrix}$$
$$+ \begin{bmatrix} 0 \\ -mgl\sin\theta \end{bmatrix} = \begin{bmatrix} 1 \\ 0 \end{bmatrix} u \tag{1}$$

These system dynamics fit the general form of the robotic manipulator equations;

$$\mathbf{H}(\mathbf{q})\ddot{\mathbf{q}} + \mathbf{C}(\mathbf{q},\dot{\mathbf{q}})\dot{\mathbf{q}} + \boldsymbol{\varphi}(\mathbf{q},\dot{\mathbf{q}}) = \mathbf{B}u \tag{2}$$

Here, $\mathbf{q}=[x\ \theta]^T$ is a configuration vector, $\mathbf{H}$ is a symmetric positive-definite mass matrix, $\mathbf{C}$ is a matrix of centripetal and Coriolis terms, $\boldsymbol{\varphi}$ is a vector of potential forces and other

generalized forces, **B** is a matrix of ones and zeros of appropriate size, and **u** is a vector of inputs to the system.
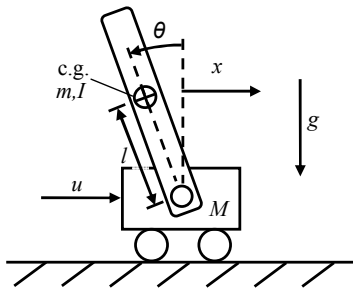

Fig. 1. Cart-pole system. The cart has mass M, and the pendulum has mass m and moment of inertia I about the c.g.

B. Swing-up controller for cart-pole

Swing-up of the cart-pole is a canonical control problem that is used to demonstrate many underactuated control algorithms. The problem is defined as applying an input force u to the cart that drives the pendulum to a neighborhood of the inverted position ($\theta = \dot{\theta} = 0$). A variant of the control problem additionally requires stabilization of the pendulum about the inverted position. This can be achieved by using a swing-up controller to drive the system into the basin of attraction of a locally stabilizing controller [9]. Another variant of the control problem involves driving the cart to the origin ($x = \dot{x} = 0$). This paper considers only the problem of swing-up.

An intuitive approach to swing-up control is based on collocated partial feedback linearization (PFL) with energy shaping [8] and is described in the following two sections.

C. Collocated Partial Feedback Linearization (PFL)

The configuration vector **q** is partitioned into collocated states $\mathbf{q}_1$ and non-collocated states $\mathbf{q}_2$, as $\mathbf{q} = \begin{bmatrix} \mathbf{q}_1^T & \mathbf{q}_2^T \end{bmatrix}^T$ depending on the actuator configuration of the system. For example, the cart-pole has an input force u acting on the cart but no input torques acting on the pendulum. As such, the cart position x is a collocated state $\mathbf{q}_1 = [x]$ and the pendulum angle θ is a non-collocated state $\mathbf{q}_2 = [\theta]$.

The manipulator equations are rewritten as follows:

$$\mathbf{H}_{11}\ddot{\mathbf{q}}_1 + \mathbf{H}_{12}\ddot{\mathbf{q}}_2 + \mathbf{C}_{11}\dot{\mathbf{q}}_1 + \mathbf{C}_{12}\dot{\mathbf{q}}_2 + \boldsymbol{\varphi}_1 = \mathbf{u} \quad (3)$$

$$\mathbf{H}_{21}\ddot{\mathbf{q}}_1 + \mathbf{H}_{22}\ddot{\mathbf{q}}_2 + \mathbf{C}_{21}\dot{\mathbf{q}}_1 + \mathbf{C}_{22}\dot{\mathbf{q}}_2 + \boldsymbol{\varphi}_2 = 0 \quad (4)$$

The non-collocated accelerations $\ddot{\mathbf{q}}_2$ are eliminated from (3), resulting in the following:

$$\mathbf{H}_{11}^*\ddot{\mathbf{q}}_1 + \mathbf{C}_{11}^*\dot{\mathbf{q}}_1 + \mathbf{C}_{12}^*\dot{\mathbf{q}}_2 + \boldsymbol{\varphi}_1^* = \mathbf{u} \quad (5)$$

$$\mathbf{H}_{11}^* = \mathbf{H}_{11} - \mathbf{H}_{12}\mathbf{H}_{22}^{-1}\mathbf{H}_{21} \quad (6)$$

$$\mathbf{C}_{11}^* = \mathbf{C}_{11} - \mathbf{H}_{12}\mathbf{H}_{22}^{-1}\mathbf{C}_{21} \quad (7)$$

$$\mathbf{C}_{12}^* = \mathbf{C}_{12} - \mathbf{H}_{12}\mathbf{H}_{22}^{-1}\mathbf{C}_{22} \quad (8)$$

$$\boldsymbol{\varphi}_1^* = \boldsymbol{\varphi}_1 - \mathbf{H}_{12}\mathbf{H}_{22}^{-1}\boldsymbol{\varphi}_2 \quad (9)$$

A reference trajectory for the collocated states $\ddot{\mathbf{q}}_{1d}(t)$ is

defined, as well as a control input **u** to drive $\ddot{\mathbf{q}}_1 \to \ddot{\mathbf{q}}_{1d}(t)$.

$$\mathbf{u} = \mathbf{H}_{11}^*\ddot{\mathbf{q}}_{1d} + \mathbf{C}_{11}^*\dot{\mathbf{q}}_1 + \mathbf{C}_{12}^*\dot{\mathbf{q}}_2 + \boldsymbol{\varphi}_1^* \quad (10)$$

This yields a hierarchical system, in which the desired accelerations of the collocated states serve as inputs to the non-collocated states, provided that there is sufficient "inertial coupling" in the $\mathbf{H}_{21}$ matrix:

$$\ddot{\mathbf{q}}_1 = \ddot{\mathbf{q}}_{1d}(t) \quad (11)$$

$$\mathbf{H}_{22}\ddot{\mathbf{q}}_2 + \mathbf{C}_{21}\dot{\mathbf{q}}_1 + \mathbf{C}_{22}\dot{\mathbf{q}}_2 + \boldsymbol{\varphi}_2 = -\mathbf{H}_{21}\ddot{\mathbf{q}}_{1d}(t) \quad (12)$$

For the cart-pole, the collocated PFL yields the following:

$$\ddot{x} = \ddot{x}_d(t) \quad (13)$$

$$(I + ml^2)\ddot{\theta} - mgl\sin\theta = ml\cos\theta\,\ddot{x}_d(t) \quad (14)$$

While an input to the pendulum is not directly available, the cart can be forced to track an arbitrary reference trajectory $\ddot{x}_d(t)$, which serves as an input to the pendulum dynamics.

D. Energy shaping

Energy shaping is an intuitive technique that can be used to drive a certain class of systems toward an unstable fixed point. For some systems, the homoclinic orbit leading to an unstable fixed point is a constant energy curve. By regulating the energy of the system to the energy of the system at the unstable fixed point, it will be driven to the homoclinic orbit and thus to the unstable fixed point.

The energy shaping controller for a class of systems given by (11-12) is derived below. The requirements are that $\mathbf{C}_{21}$ has no nonzero elements, $\boldsymbol{\varphi}_2$ is not a function of $\mathbf{q}_1$ or $\dot{\mathbf{q}}_1$, and $\boldsymbol{\varphi}_2$ consists only of passive generalized forces and conservative forces. Under these conditions, the non-collocated dynamics given in (12) can be interpreted as a virtual subsystem with energy given as:

$$E = \frac{1}{2}\dot{\mathbf{q}}_2^T\mathbf{H}_{22}\dot{\mathbf{q}}_2 + V(\mathbf{q}_2) \quad (15)$$

The desired energy level corresponding to the system energy at the unstable fixed point and its homoclinic orbit is defined as E_d. The error between current energy and desired energy is defined as:

$$\widetilde{E} = E - E_d \quad (16)$$

The energy-shaping controller is then defined by finding a control law for $\ddot{\mathbf{q}}_{1d}(t)$ that drives the energy error $\widetilde{E}$ to 0. Such a controller for the cart-pole is presented below.

For the cart-pole, the system energy, desired energy at tip-up, and time derivative of energy are given as:

$$E = \frac{1}{2}(I + ml^2)\dot{\theta}^2 + mgl\cos\theta \quad (17)$$

$$E_d = mgl \quad (18)$$

$$\dot{E} = \dot{\theta}\,ml\cos\theta\,\ddot{x}_d \quad (19)$$

A state vector $\mathbf{x} = \begin{bmatrix} \mathbf{q}_2^T & \dot{\mathbf{q}}_2^T \end{bmatrix}^T$ is defined along with an autonomous Lyapunov-like function $V(\mathbf{x})$ for the energy shaping controller.

$$V(\mathbf{x}) = \frac{1}{2}\widetilde{E}^2 \qquad (20)$$

A control law is proposed below, where $K_1 > 0$, along with a corresponding value for $\dot{V}$.

$$\ddot{x}_d = -K_1 \widetilde{E} \dot{\theta} \cos\theta \qquad (21)$$

$$\dot{V} = -K_1 m l \widetilde{E}^2 \dot{\theta}^2 \cos^2\theta \leq 0 \qquad (22)$$

Barbalat's lemma can show that this controller will drive the system to the largest invariant set for which $\dot{V} = 0$. This invariant set includes the homoclinic orbit ($\widetilde{E} = 0$) and the equilibrium points of the pendulum ($\sin\theta = 0$, $\dot{\theta} = 0$). The controller can be modified to drive the pendulum away from its downward equilibrium point with the switching controller given below, using a sgn function that returns only nonzero values (ie. sgn(0) = 1):

$$E_0 = mgl\cos\theta_0 \qquad \cos\theta_0 < 0 \qquad (23)$$

$$\ddot{x}_d = \begin{cases} -K_1 \widetilde{E} \dot{\theta} \cos\theta & E > E_0 \\ -K_2 \operatorname{sgn}\dot{\theta} & E \leq E_0 \end{cases} \qquad (24)$$

Results and further discussion of this type of controller for the cart-pole can be found in [8, 9].

III. VEHICLE ROLLOVER DYNAMICS

A. Comparison to cart-pole dynamics

Vehicle rollover can occur when lateral forces acting at the tires cause the wheels on one side of the vehicle to lift off the ground and the c.g. to rotate up to an unstable equilibrium point directly above the other set of wheels. If the vehicle is modeled as a single rigid body, the angle θ is defined as the angle between the c.g. and the vertical as shown in Fig. 2, and the unstable equilibrium point corresponds to $\theta = 0$. In this case, the vehicle is equivalent to a cart-pole system with a massless cart, as illustrated in the right subfigure of Fig. 2.
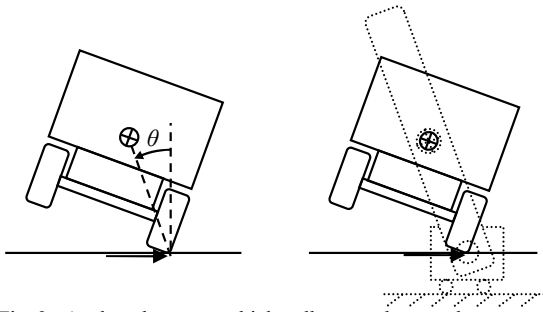

Fig. 2. Analogy between vehicle rollover and cart-pole.

It is important to mention several distinct differences between the cart-pole and rigid body vehicle. The first is that the cart and pole are connected by a pin joint, while the vehicle is held against the ground by a non-negative contact force N, given below:

$$N = mg - ml\left(\ddot{\theta}\sin\theta + \dot{\theta}^2\cos\theta\right) \qquad (25)$$

If the contact force N goes to zero, the vehicle dynamics will differ from the cart-pole and become ballistic.

The second difference is an intuitive physical limit on the input force acting at the tires. Since the tire input force is generated by friction, it is assumed that the magnitude of the tire frictional forces is limited by the following equation, where μ is the friction coefficient and N is given above:

$$-\mu N \leq u \leq \mu N \qquad (26)$$

The force vector consisting of both the frictional input force u and the normal force N makes an angle α with the vertical, as shown in Fig. 3. The constraint in (26) can be interpreted as a limit of the magnitude of α to be less than $\tan^{-1}\mu$ and thus to point between the dashed lines in Fig. 3. This limitation is often referred to as the friction cone [11].

It can be shown that if the vehicle c.g. lies outside the friction cone ($\theta > \tan^{-1}\mu$), as in the left subfigure of Fig. 3, all physically attainable forces will accelerate the vehicle away from tip-up towards the ground. In this case, there is insufficient friction to achieve tip-up. If the c.g. lies within the friction cone ($\theta \leq \tan^{-1}\mu$), however, then contact forces can be applied to accelerate the vehicle towards tip-up. This relation between the surface friction and c.g. position constitutes a necessary condition for tip-up [12]. A crucial parameter to note is the height of the vehicle c.g. Increasing this value reduces the friction coefficient needed for tip-up, making tip-up easier.
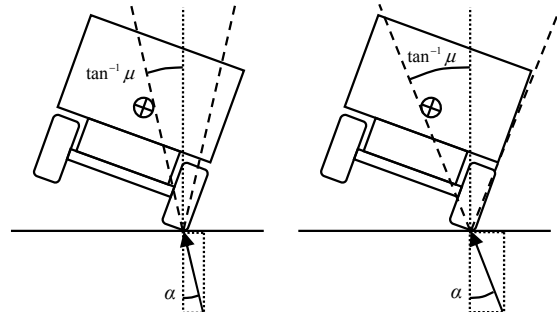

Fig. 3. Friction cone and vehicle c.g. position. Left: Case where tip-up is impossible. Right: Case where tip-up is possible.

It should also be mentioned that there are no practical actuators for directly generating lateral tire forces. Lateral tire forces are typically modeled as functions of lateral slip, which may be controlled by steering, and longitudinal slip, which may be controlled by tractive or braking force [4, 5]. In this paper, the lateral tire friction force is treated as an input, which assumes the existence of a separate force controller based on steering and tractive or braking force. In practice, such controllers would have limited bandwidth and possibly other trajectory-dependent limitations. These effects are not considered in this paper but are a topic of future work.

The similarity between vehicle rollover dynamics and cart-pole dynamics suggests that control algorithms used to swing up and stabilize the cart-pole may be applicable for tip-up and stabilization of a vehicle near rollover.

B. Vehicle model with suspension dynamics

The analogy between the cart-pole and a rigid body

vehicle near rollover made in the previous section neglects the effect of the vehicle's suspension dynamics, which have a significant impact on vehicle rollover [13]. Here a multi-body vehicle model with suspension effects is proposed with a corresponding energy-based controller. Note that energy shaping methods have been successfully applied to systems such as a double inverted pendulum on a cart [14], which have similarity to the multi-body system presented here.

The model consists of the vehicle body connected to a solid axle with a revolute joint at point b. The body c.g. and axle c.g. are located at point c and point b respectively. The equations of motion for the model depend on the wheel contact conditions, denoted LR when both left and right wheels are on the ground, L when only left wheels are on the ground, R when only right wheels are on the ground, and N when no wheels are on the ground. Conditions LR and L are illustrated in Fig. 4 below.
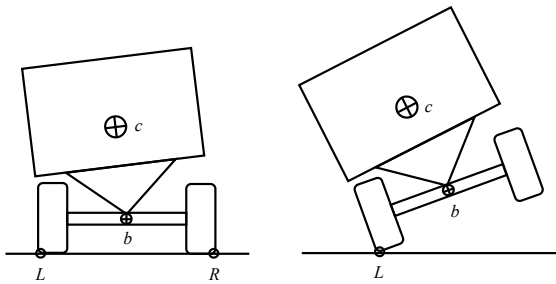

Fig. 4. Vehicle model with pin joint suspension and solid axle. Left: Contact mode LR. Right: Contact mode L.

The vehicle model can be formulated as a multi-link manipulator as illustrated in Fig. 5 with angles q_a and q_b. The axle is modeled as a link with a constant offset angle q_0, link length l_a, mass m_a, and moment of inertia I_a. The vehicle body is modeled as a link with length l_b, mass m_b, and moment of inertia I_b. The total mass of the system is $M = m_a + m_b$. The effect of springs, hardstops, and dampers in the suspension is modeled as a torque τ acting between the axle and vehicle body. The torque has a stiffness coefficients k_1, k_3, and k_5, and damping b_1 and is given as:

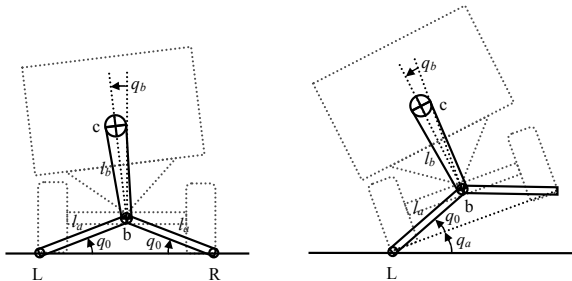$$\tau = -k_1 q_b - k_3 q_b^3 - k_5 q_b^5 - b_1 \dot{q}_b \tag{27}$$

Fig. 5. Vehicle model as multi-link manipulator. Left: Contact mode LR. Right: Contact mode L.

The states and kinematics for each contact condition are given in Table I and (28) below using the following notation:

$s_i \equiv \sin q_i$, $s_{i+j} \equiv \sin(q_i + q_j)$, $s_{i-j} \equiv \sin(q_i - q_j)$,

$c_i \equiv \cos q_i$, $c_{i+j} \equiv \cos(q_i + q_j)$, and $c_{i-j} \equiv \cos(q_i - q_j)$.

TABLE I
STATES AND KINEMATICS OF EACH CONTACT MODE

Mode	States	Position of Point b
LR	x_{LR}, q_b	$\begin{bmatrix} x_b \\ y_b \end{bmatrix}_{LR} = \begin{bmatrix} x_{LR} \\ 0 \end{bmatrix} + l_1 \begin{bmatrix} 0 \\ s_0 \end{bmatrix}$
L	x_L, q_a, q_b	$\begin{bmatrix} x_b \\ y_b \end{bmatrix}_L = \begin{bmatrix} x_L \\ 0 \end{bmatrix} + l_1 \begin{bmatrix} c_{0+a} \\ s_{0+a} \end{bmatrix}$
R	x_R, q_a, q_b	$\begin{bmatrix} x_b \\ y_b \end{bmatrix}_R = \begin{bmatrix} x_R \\ 0 \end{bmatrix} + l_1 \begin{bmatrix} -c_{0-a} \\ s_{0-a} \end{bmatrix}$
N	x_N, y_N, q_a, q_b	$\begin{bmatrix} x_b \\ y_b \end{bmatrix}_N = \begin{bmatrix} x_N \\ y_N \end{bmatrix}$

$$\begin{bmatrix} x_c \\ y_c \end{bmatrix}_i = \begin{bmatrix} x_b \\ y_b \end{bmatrix}_i + l_2 \begin{bmatrix} -s_{a+b} \\ c_{a+b} \end{bmatrix} \tag{28}$$

The equations of motion for each contact mode fit the form of the manipulator equations in (2). The matrices for contact mode L are provided below.

$$H_{12L} = -Ml_a s_{0+a} - m_b l_b c_{a+b} \tag{29}$$

$$H_{22L} = I_a + Ml_a^2 + I_b + m_b l_b^2 + 2m_b l_a l_b s_{0-b} \tag{30}$$

$$H_{23L} = I_b + m_b l_b^2 + m_b l_a l_b s_{0-b} \tag{31}$$

$$\mathbf{H}_L = \begin{bmatrix} M & H_{12L} & -m_b l_b c_{a+b} \\ H_{12L} & H_{22L} & H_{23L} \\ -m_b l_b c_{a+b} & H_{23L} & I_b + m_b l_b^2 \end{bmatrix} \tag{32}$$

$$C_{12L} = -Ml_a c_{0+a} \dot{q}_a + m_b l_b s_{a+b}(\dot{q}_a + \dot{q}_b) \tag{33}$$

$$\mathbf{C}_L = \begin{bmatrix} 0 & C_{12L} & m_b l_b s_{a+b}(\dot{q}_a + \dot{q}_b) \\ 0 & -m_b l_a l_b c_{0-b} \dot{q}_b & -m_b l_a l_b c_{0-b}(\dot{q}_a + \dot{q}_b) \\ 0 & m_b l_a l_b c_{0-b} \dot{q}_a & 0 \end{bmatrix} \tag{34}$$

$$\boldsymbol{\varphi}_L = \begin{bmatrix} 0 \\ Mgl_a c_{0+a} - m_b gl_b s_{a+b} \\ -\tau - m_b gl_b s_{a+b} \end{bmatrix} \tag{35}$$

$$\mathbf{B}_L = \begin{bmatrix} 1 & 0 & 0 \end{bmatrix}^T \tag{36}$$

As a system with multiple dynamic modes, there must be logic for switching between the modes, which is given in Table II. Any collisions that occur during mode transitions are assumed to be inelastic collisions. Note that N_L and N_R represent the sum of normal forces acting on the left and right sides of the vehicle. The equations used to compute N_L and N_R during mode L are given below.

$$N_L = Mg + Ml_a c_{0+a} \ddot{q}_a - m_b l_b s_{a+b}(\ddot{q}_a + \ddot{q}_b) \\ - Ml_a s_{0+a} \dot{q}_a^2 - m_b l_b c_{a+b}(\dot{q}_a + \dot{q}_b)^2 \tag{37}$$

$$N_R = 0 \tag{38}$$

TABLE II
CONDITIONS FOR TRANSITIONING BETWEEN CONTACT MODES

	to LR	to L	to R	to N
from LR	—	$N_R = 0$	$N_L = 0$	$N_L = N_R = 0$
from L	$q_a = 0$	—	$q_a = N_L = 0$	$N_L = 0$
from R	$q_a = 0$	$q_a = N_R = 0$	—	$N_R = 0$
from N	$y_L = y_R = 0$	$y_L = 0$	$y_R = 0$	—

C. Tip-up controller for vehicle rollover model

A tip-up controller for the vehicle rollover model is designed using partial feedback linearization and energy shaping in a similar manner to the swing up controller designed for the cart-pole in Sections II. *B*. and *C*. The partial feedback linearization is computed directly using (5)-(12) and the manipulator matrices for contact modes *LR*, *L*, and *R*. No controller is derived for mode *N* since there is no input in this mode.

An energy shaping control law similar to (21)-(22) is presented here. Recalling that $\mathbf{q}_2$ is the vector of non-collocated states for each contact mode, the potential energy and total energy of the non-collocated subsystem for the vehicle model are:

$$V(\mathbf{q}_2) = m_a g y_b + m_a g y_c + \frac{1}{2} k_1 q_b^2 + \frac{1}{4} k_3 q_b^4 + \frac{1}{6} k_5 q_b^6 \qquad (39)$$

$$E = \frac{1}{2} \dot{\mathbf{q}}_2^T \mathbf{H} \dot{\mathbf{q}}_2 + V(\mathbf{q}_2) \qquad (40)$$

The configuration angles $\hat{\mathbf{q}}_2$ of the vehicle at tip-up equilibrium are computed numerically from the following:

$$\boldsymbol{\varphi}_L(\hat{\mathbf{q}}_2, \mathbf{0}) = \mathbf{0} \qquad (41)$$

The desired energy at tip-up E_d is computed from this equilibrium state as follows:

$$E_d = V(\hat{\mathbf{q}}_2) \qquad (42)$$

Recalling the state vector definition $\mathbf{x} = \begin{bmatrix} \mathbf{q}_2^T & \dot{\mathbf{q}}_2^T \end{bmatrix}^T$ and the Lyapunov-like function in (20), a control law and associated $\dot{V}$ is presented, where $K > 0$:

$$\ddot{\mathbf{q}}_{1d} = K \widetilde{E} \mathbf{H}_{21}^T \dot{\mathbf{q}}_2 \qquad (43)$$

$$\dot{V} = -b_1 \dot{q}_b^2 \widetilde{E} - K \widetilde{E}^2 \dot{\mathbf{q}}_2^T \mathbf{H}_{21} \mathbf{H}_{21}^T \dot{\mathbf{q}}_2 \qquad (44)$$

It is seen in (44) that for large values of $\widetilde{E}$, the right-hand quadratic term will dominate the expression and $\dot{V}$ will be negative. This means that $\widetilde{E}$ is being driven to zero as desired. However, the energy dissipation term $-b_1 \dot{q}_b^2 \widetilde{E}$ could be positive for $\widetilde{E} > 0$, and thus $\dot{V}$ could be positive for small values of $\widetilde{E}$. Thus there is a small region of error near the desired energy state where $\dot{V}$ is indefinite. This region is easily adjusted by modifying the positive gain *K*.

There are several other issues with this control design that must be noted. The first is the limitations on the input force by the available friction, which will prevent convergence of the energy to the desired value when insufficient friction is available. A second issue is an energy dissipation mechanism that is not considered in the Lyapunov analysis, which is the energy lost from inelastic collisions with the ground. Given sufficient friction to overcome the energy dissipation mechanisms, the controller will drive the vehicle to a tip-up condition.

IV. SIMULATION RESULTS

A. Setup

The controller derived in III. *C*. was simulated with the vehicle model from III. *B*. and the model parameters given in Table III.

TABLE III
VEHICLE MODEL PARAMETERS

Description	Symbol	Value
Axle mass	m_1	160 kg
Body mass	m_2	1870 kg
Total mass	M	2030 kg
Axle inertia	I_1	102 kg m^2
Body inertia	I_2	1240 kg m^2
Axle angle offset	q_0	0.124 rad
Link 1 length	l_1	0.806 m
Link 2 length	l_2	0.500 m
Linear stiffness	k_1	7.49 x 10^4 Nm / rad
3rd order stiffness	k_3	0 Nm / rad^3
5th order stiffness	k_5	2.7 x 10^7 Nm / rad^5
Linear damping	b_1	3200 Nm / (rad/s)

B. Results: high friction (μ=1.50)

The first set of simulation results demonstrate the successful tip-up of a vehicle on a surface with a friction coefficient $\mu = 1.50$. The vehicle state is illustrated at several instants in Fig 6. The friction cone is plotted for each wheel contact point, and the lumped c.g. of the system is represented by a dark circle. It can be seen that the lumped c.g. lies within the friction cones from time *t*=0, which enables tip-up.

The phase plane trajectories of the lumped c.g. inclination angle θ for both the left and right contact points are shown in Fig. 7. The friction cone angle is represented with a solid line. It can be seen that the system approaches the unstable equilibrium point at (0,0).
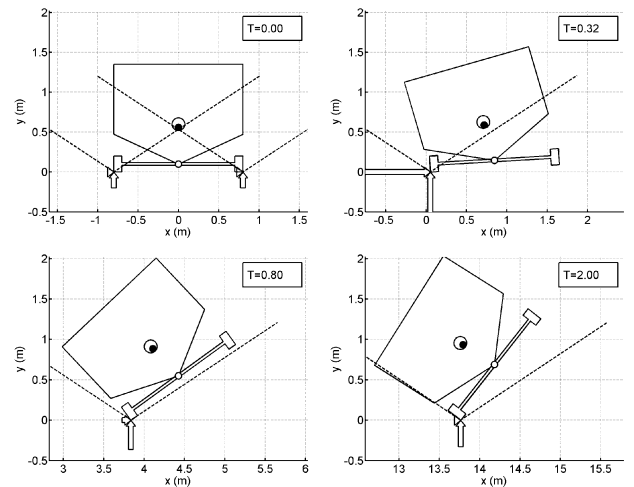

Fig. 6. Snapshots of vehicle orientation during tip-up simulation with friction coefficient of $\mu = 1.50$.

Plots of the system energy and the input force *u* are given in Figs. 8 and 9. It can be seen that the system energy converges to the desired energy level in less than 0.5 s. Note that the maximum allowable input force depends on the normal forces, which can vary dynamically.
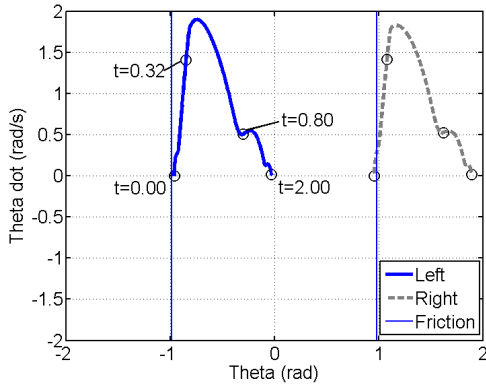
Fig. 7. Phase plane trajectory of θ vs. $\dot{\theta}$ for c.g. position relative to left and right wheels for tip-up simulation with friction coefficient of $\mu = 1.50$. The friction cone angle $\tan^{-1}\mu$ is shown with a solid line.
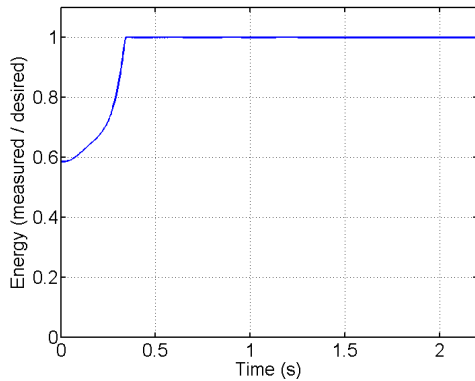

Fig. 8. Energy of non-collocated states during tip-up simulation with friction coefficient of $\mu = 1.50$.
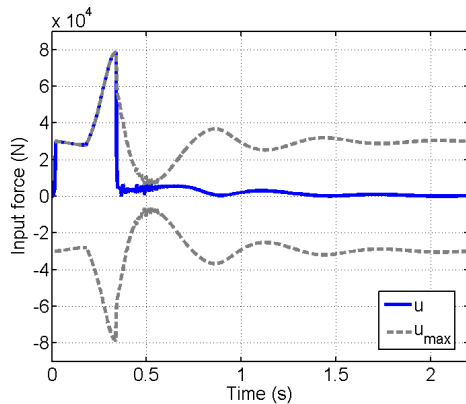

Fig. 9. Input force during tip-up simulation with friction coefficient of $\mu = 1.50$.

C. Results: lower friction ($\mu=1.00$)

The second set of simulation results demonstrates a successful tip-up on a surface with friction coefficient of 1.00, illustrated with snapshots in Fig. 10 and phase plane trajectories in Fig. 11.

The vehicle c.g. initially lies outside the friction cones and does not reach tip-up on the first force input. Some momentum is subsequently transferred, and during the second push (in the opposite direction from the first) the c.g. is driven into the friction cone and proceeds to tip-up.
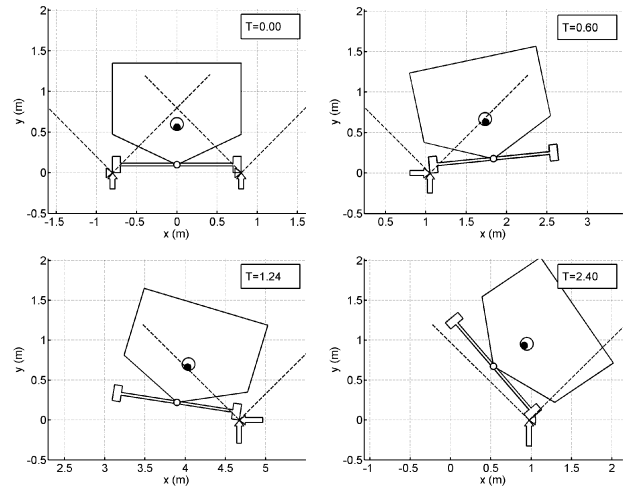

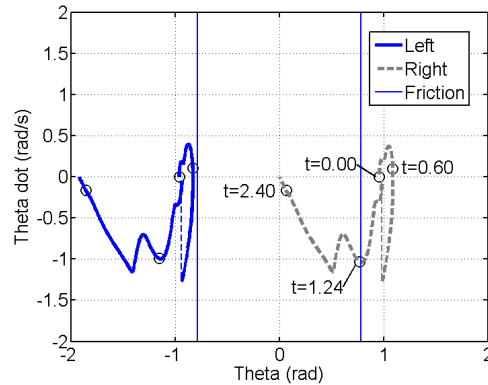Fig. 10. Snapshots of vehicle orientation during tip-up simulation with friction coefficient of $\mu =1.00$.

Fig. 11. Phase plane trajectory of θ vs. $\dot{\theta}$ for left and right wheels for tip-up simulation with friction coefficient of $\mu = 1.00$. The friction cone angle $\tan^{-1}\mu$ is shown with a solid line.

Plots of the system energy and input force u are given in Figs. 12 and 13. Note that a change of contact state (from L to LR) occurs at t=0.78, which results in an inelastic collision. This causes discontinuities in the $\dot{\theta}$ terms in Fig. 11, the system energy in Fig. 12 and the available input force in Fig. 13.
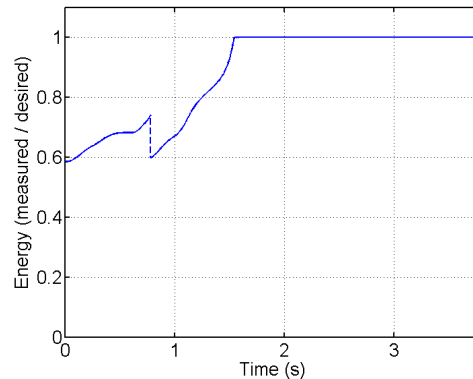

Fig. 12. Energy of non-collocated states during tip-up simulation with friction coefficient of $\mu = 1.00$.
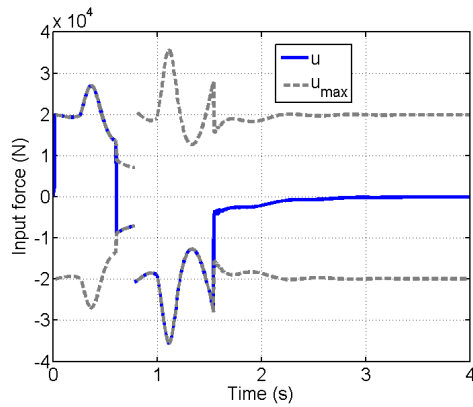
Fig. 13. Input force with friction coefficient of $\mu = 1.00$.

D. Discussion

In these results, the controller successfully drives the vehicle to tip-up with markedly different trajectories. In each case, the controller attempts to drive the system energy to the desired value by pushing in a direction defined by the term $\widetilde{E}\,\mathbf{H}_{21}^{T}\dot{\mathbf{q}}_2$ from (42). In the first case, the vehicle c.g. was initially within the friction cone, so that the vehicle was able to reach tip-up without the term $\widetilde{E}\,\mathbf{H}_{21}^{T}\dot{\mathbf{q}}_2$ changing sign. In the second case, however, the term $\widetilde{E}\,\mathbf{H}_{21}^{T}\dot{\mathbf{q}}_2$ changed signs prior to reaching the desired energy level. This caused the controller to pump energy into the system by pushing in the opposite direction and eventually reach the desired value. Although energy was lost during the impact at the contact mode transitions, it did not prevent the build up of energy over two "pumps." Given appropriate system parameters and initial conditions, it is likely possible to generate tip-up trajectories with this controller using any number of "pumps."

The potential of this controller to drive the vehicle to tip-up is highly dependent on the system parameters, especially the relationship between friction coefficient and c.g. position. When the c.g. is initially outside the friction cone, the parameters affecting energy dissipation become important.

V. CONCLUSION

An analogy between the dynamics of the cart-pole and a vehicle near rollover has been drawn, and it has been shown that a controller for swinging up the cart-pole to an inverted position can be employed to tip up a vehicle near rollover. The model considers suspension effects and surface friction, which limits the magnitude of the input force, but does not consider the vehicle steering or yaw dynamics, which in practice would limit the input bandwidth. Future work will consider a 3D vehicle model with yaw and steering dynamics and possibly use open-loop trajectory optimization to determine the range of suspension parameters and friction values that permit tip-up stabilization.

REFERENCES

[1] National Highway Traffic Safety Administration (NHTSA). DOT HS 809 919. Traffic Safety Facts 2004: A Compilation of Motor Vehicle Crash Data from the Fatality Analysis Reporting System and the General Estimates System.

[2] D. Odenthal, T. Bunte and J. Ackermann, "Nonlinear steering and braking control for vehicle rollover avoidance", *Proc. European Control Conf.*, Karlsruhe, Aug. 31 - Sept. 3, 1999.

[3] B. Chen, H. Peng, "Differential-Braking-Based Rollover Prevention for Sport Utility Vehicles with Human-in-the-loop Evaluations," *Vehicle System Dynamics*, v. 36, n. 4&5, pp. 359-389, 2001.

[4] C. R. Carlson and C. J. Gerdes, "Optimal rollover prevention with steer by wire and differential braking," *Proc. ASME Dynamic Systems and Control Division - 2003*, pp. 345-354, November 2003.

[5] B. Johansson, M. Gafvert, "Untripped SUV rollover detection and prevention," *Proc. 43rd IEEE Conf. Decision and Control, 2004*, v. 5, pp. 5461-5466, 2004.

[6] S. Choi, "Practical vehicle rollover avoidance control using energy method," *Vehicle System Dynamics*, v. 46, n. 4, pp. 323-337, 2008.

[7] J. Lu, D. Messih, A. Salib, "Roll Rate Based Stability Control - the Roll Stability Control System," *Proc. of 20th Intl. Technical Conf. on the Enhanced Safety of Vehicles*, NHTSA, n. 07-136, pp. 1-13, 2007.

[8] M. W. Spong, "Energy Based Control of a Class of Underactuated Mechanical Systems," *1996 IFAC World Congress*, San Francisco, CA, July, 1996.

[9] M. W. Spong, L. Praly, "Control of underactuated mechanical systems using switching and saturation," *Control Using Logic-Based Switching*, Ed. S. Morse, Springer Berlin / Heidelberg, 1997, pp. 162-172.

[10] G. A. Sohl, J. E. Bobrow, "A Recursive Multibody Dynamics and Sensitivity Algorithm for Branched Kinematic Chains," *Journal of Dynamic Systems, Measurement, and Control*, v. 123, n. 3, pp. 391-399, 2001.

[11] C. A. Klein, S. Kittivatcharapong, "Optimal force distribution for the legs of a walking machine with friction cone constraints," *IEEE Trans. on Robotics and Automation*, v. 6, n. 1, pp. 73-85, Feb. 1990.

[12] S. C. Peters, "Modeling, Analysis, and Measurement of Passenger Vehicle Stability," M.S. thesis, Massachusetts Institute of Technology, Dept. of Mech. Engr., Cambridge, MA, September 2006.

[13] A. Hac, "Rollover Stability Index Including Effects of Suspension Design," *SAE Transactions*, n. 2002-01-0965, 2002.

[14] W. Zhong, H. Rock, "Energy and passivity based control of the double inverted pendulum on a cart," *Proc. of the 2001 IEEE Intl. Conf. on Control Applications*, pp. 896-901, 2001.